Si–N–O Films Synthesized by Plasma Immersion Ion Implantation and Deposition (PIII&D) for Blood-Contacting Biomedical Applications

Guo Jiang Wan, N. Huang, Sunny C. H. Kwok, Zh. Y. Shao, A. S. Zhao, P. Yang, and Paul K. Chu, *Fellow, IEEE*

***Abstract*—Silicon-Oxynitride (Si–N–O) films were fabricated on silicon wafers by silicon cathodic arc combined with plasma immersion ion implantation and deposition. The blood compatibility of the films was assessed by platelet-adhesion test and fibrinogen conformational change measurements to evaluate the viability of the materials in biomedical engineering. Significantly, a better platelet-adhesion behavior, as manifested by a smaller number and weaker aggregation as well as pseudopodium, was observed on the Si–N–O samples compared to the low-temperature isotropic pyrolytic carbon, which is the most common material used in blood-contacting biomedical devices such as artificial heart valves. Enzyme-linked-immunoassay measurements that disclose fibrinogen conformational changes show results that are consistent with the platelets' behavior, which is believed to be involved in the activation process. The good blood compatibility of the films can be attributed to the high hydrophilicity and surface free energy arising from the Si–N, Si–N–O, and Si–O bonding states. The interfacial reactions between fibrinogen, platelets, and material surface are discussed from the perspective of thermodynamics. The promising blood compatibility of the Si–N–O films is of both scientific and commercial interests in biomedical engineering.**

***Index Terms*—Films, implantable biomedical devices, plasma materials-processing applications, silicon compounds, surface treatment.**

I. Introduction

SILICON-OXYNITRIDE (Si–N–O) films possess the properties of both silicon nitride and silicon oxide [1]. The materials are used extensively in microelectronics, optoelectronics, and solar cells, as they are very good protective layers against wear and corrosion and can also be used as thin dielectric membranes, insulating barriers, and so on [1], [2]. It has also been recently shown that silicon-oxynitride films are potentially attractive biomaterials in dental applications [3], joint or pH-ISFET biosensors [4], bioMEMS [5], and other applications [6]–[8]. For instance, nitrogen/ammonia plasma immersion ion implantation (PIII) has been used to produce silicon-oxynitride films and their biological properties have been evaluated [9], [10]. In some applications, deposited films are more preferred because of the existence of a distinctive interface with the substrate. Many techniques have been employed to synthesize silicon-oxynitride thin films, such as chemical vapor deposition (CVD), jet VD (JVD), atomic layer deposition (ALD), and plasma nitriding [1], [2]. It is generally accepted that different methods produce silicon-oxynitride films with different structural and physiochemical properties. Recently, we employed silicon cathodic arc in concert with PIII and deposition (PIII&D) to produce Si-doped diamondlike carbon (DLC) films [11]. The combined use of cathodic arc and PIII&D offers a number of advantages such as pure silicon plasma, high ionization efficiency, easy control of the implantation/deposition parameters by adjustment of the bias voltage on the fly, and non-line-of-sight operation, thereby making the technique especially attractive for biomedical components and implants possessing complex shapes [12]. In this paper, we report the synthesis of Si–N–O films synthesized by this hybrid technique and the blood compatibility of the materials to evaluate the viability in long-term invasive blood-contacting applications [13], [14].

Manuscript received November 11, 2005; revised March 28, 2006. This work was supported by the Hong Kong Research Grants Council (RGC) and by NSFC Joint Scheme N_CityU101/03 as well as NSFC 30570502 of China.

G. J. Wan is with the Key Laboratory of Advanced Technology for Materials (China Education Ministry), College of Materials Science and Engineering, Southwest Jiaotong University, Chengdu 610031, China, and also with the Department of Physics and Materials Science, City University of Hong Kong, Hong Kong (e-mail: superwgj@263.net; Namba_WAN@home.swjtu.edu.cn).

N. Huang, Zh. Y. Zhao, A. S. Zhao, and P. Yang are with the Key Laboratory of Advanced Technology for Materials (China Education Ministry), College of Materials Science and Engineering, Southwest Jiaotong University, Chengdu 610031, China.

S. C. H. Kwok and P. K. Chu are with the Department of Physics and Materials Science, City University of Hong Kong, Hong Kong (e-mail: paul.chu@cityu.edu.hk).

Digital Object Identifier 10.1109/TPS.2006.881509

II. Experimental Details

A. Si–N–O Film Deposition

Deposition was conducted on p-type (100) silicon wafers in our PIII&D instrument equipped with four cathodic-arc sources [15]. The silicon plasma was generated by one of the cathodic-arc source composed of a high-purity (99.999%) silicon cathode. The instrumental parameters are listed in Table I. The silicon plasma drifted through a 90° curved magnetic duct to eliminate deleterious macroparticles and then impacted the silicon substrate biased at -200 V dc. Concurrently, nitrogen, oxygen, or ammonia gas was selectively bled into the PIII&D chamber (base pressure: 4.0×10^{-3} Pa) at the vicinity of the metal arc discharge plume from the top of the processing chamber. The cathodic silicon arc was triggered, and the streaming silicon plasma also collided with the gas molecules, causing partial ionization. The films were deposited

TABLE I
Si CATHODIC-ARC SOURCE AND PIII&D INSTRUMENTAL CONDITIONS

Sample Number	$F_{O2/N2/NH3}$ (SCCM)	Working Pressure (Pa)	Bias Voltage (Volt.)	Silicon Arc source		Deposition time (min.)
				Trigger Voltage	Main arc current	
# 1	O_2/N_2(5/20)	1.2×10^{-1}	-200 (DC)	3 kV	120A (250μs, 60Hz)	90
# 2	N_2 (25)	1.1×10^{-1}				
# 3	NH_3(20)	1.1×10^{-1}				

by the reaction of ionized silicon with the gas plasma and gas molecules. According to our previous experiments [9], oxygen can compete strongly with nitrogen to react with silicon, and ammonia can be more readily ionized, thereby improving the nitrogen retained dose. As a result, we selected the instrumental conditions summarized in Table I.

B. Characterization

The composition and chemical states of the films in the near-surface region ($\sim$ 10 nm) were determined by X-ray photoelectron spectroscopy (XPS, PHI 5600) using a monochromatic Al K_α X-ray source. The structural bonding states of the film were characterized by Fourier transform infrared spectroscopy (FTIR) on a Perkin-Elmer 1600. The film/substrate morphology was observed by cross-sectional filed-emission scanning electron microscope (FEG SEM, JEOL, JSM-6335F).

The hydrophilicity was determined by a contact-angle test using the sessile drop method on the JY-82 contact-angle goniometer in ambient condition. The surface free energy, including the surface tension γ_s and its polar γ^p and dispersive γ^d components, was calculated by the contact-angle data measured on the sample surface with six different electrolytes (double distilled water, glycerin, formamide, diiodomethane, glycol, and tritolyl phosphate). The details of this method and calculation can be found elsewhere [11], [16]. Ten measurements were made on each sample to obtain good statistics.

C. Blood Compatibility

The platelet-adhesion test was conducted on the Si–N–O samples as well as low-temperature isotropic pyrolytic carbon (LTIC) serving as the control [17], [18]. LTIC is the most common clinical blood-contacting biomaterials used in artificial heart valves. The cultivation time was two hours in each test. The quantity and morphology of the adherent platelets were assessed as parameters for blood compatibility using optical microscopy or scanning electron microscopy (JEOL JSE-820). Again, in order to obtain good statistics, averages of ten random-picked fields were taken from each sample.

Enzyme-linked immunoassay (ELISA) examination was employed to estimate the fibrinogen structural conformation change. Here, the fibrinogen broken γ chains are exposed to and coupled with the GPIIb-IIIa series chains of platelets, stimulating the activation of platelets [19], [20]. The first antibody (mouse antihuman fibrinogen γ chain; Accurate Chemical & Scientific Corporation) and the second antibody (goat antimouse multiantibody; Abcam Corporation) mark the extent of the fibrinogen (as antigen) transformation employing the ELISA method conducted in platelet-poor plasma (PPP). The experimental procedures can be found elsewhere [21], [22].

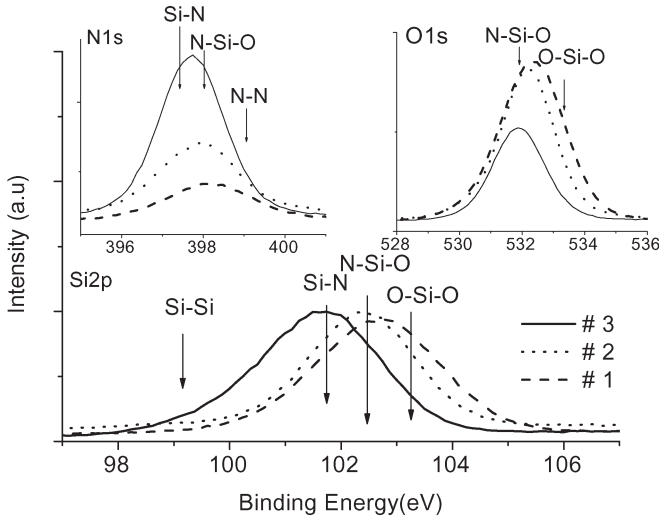

Fig. 1. Si2p, N1s, and O1s core level XPS spectra of the Si–N–O films synthesized by PIII&D.

TABLE II
SURFACE COMPOSITION OF THE Si–N–O FILMS SYNTHESIZED BY PIII&D AS DETERMINED BY XPS

Elements / samples	O (O 1s)	N (N 1s)	Si (Si 2p)	C (C 1s)
# 1	55.94	5.91	32.86	balanced
# 2	49.65	11.26	32.70	
# 3	30.88	22.29	41.15	

III. RESULTS AND DISCUSSION

The surface chemical states revealed by the Si2p, N1s, and O1s photoelectron peaks are shown in Fig. 1, and the elemental compositions calculated from the XPS core level peaks are listed in Table II. More nitrogen is incorporated with an increasing nitrogen partial pressure, using ammonia as the precursor. The oxygen contents are relatively high in all the samples because of the strong affinity of oxygen to silicon during deposition [9]. According to the values calculated from the XPS core level peaks shown in Table II, at our base pressure,

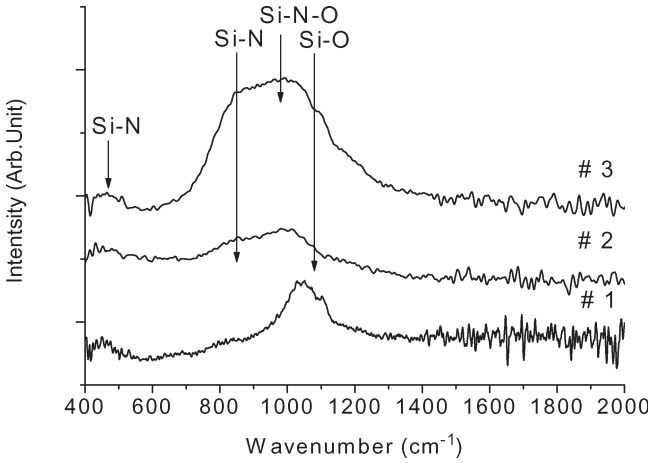

Fig. 2. FTIR absorbance spectra acquired from the PIII&D Si–N–O films.

the nitrogen content can be higher than 11% (sample #2) if nitrogen is used as the precursor and more than 22% (sample #3) when ammonia is employed as the precursor, whereas it is much less at $\sim$ 5% (sample #1) when oxygen gas is used. The nitrogen content can thus be obtained effectively using our hybrid technique, as suggested in [2]. The relative peak intensities and binding energy shifts (calibrated by the C1s peak value of 284.8 eV [23]) of the Si2p, N1s, and O1s peaks reveal this consistent change. In the Si2p spectra, an obvious lower energy shift can be seen from samples #1 to #3, confirming the configuration changes from dominantly Si–O to Si–N–O and Si–N bonding states with increasing nitrogen incorporation [23]. In fact, all Si2p peaks acquired from the three samples can be deconvoluted into bonding components, including one at $\sim$ 103.3 eV, which is indicative of Si–O, one at a lower energy ($\sim$ 102.4 eV), which is attributable to Si–N–O, and a Si–N component at $\sim$ 101.8 eV [24]. The N1s photoelectron peak results confirm the tendency. The peak around 396.9 eV can be attributed to Si–N, and the one at approximately 397.4 eV arises from Si–N–O [25]. A similar trend can be observed for the O1s photoelectron peak showing the existence of Si–O ($\sim$ 533.2 eV) and Si–N–O ($\sim$ 531.9 eV) in samples #1 and #2, but much less in sample #3.

Fig. 2 depicts the FTIR absorbance spectra acquired from the samples. One broad peak appears from sample #1 from 1000 to 1100 cm^{-1}, as a proof of the Si–O stretching vibration. The lower frequency shoulder can be assigned to Si–N–O ($\sim$ 980 cm^{-1}), and another small peak at about 845 cm^{-1} is the Si–N stretching mode [26], [27]. A broad absorption band from 700 to 1200 cm^{-1} can be observed from samples #2 and #3, and it can be deconvoluted into a peak centered at approximately 845 cm^{-1}, corresponding to the asymmetric in-plane Si–N stretching vibration mode, with one at around $900-1000$ cm^{-1}, which is attributable to Si–N–O, and another one at 1050 cm^{-1} for Si–O [26], [27]. Complete deconvolution of the broadband is not easy and remains controversial due to the complexity of oxygen coordination with nitrogen and silicon as well as the different sensitivity factors of different bonding states [26]. Nonetheless, the observed peak intensities and vibration frequency shifts corroborate the bonding-state changes. No obvious peaks of Si–H and N–H appear from sample #3 in the FTIR spectra in the range of $400-4000$ cm^{-1}, indicating negligible hydrogen incorporation in our experiments.

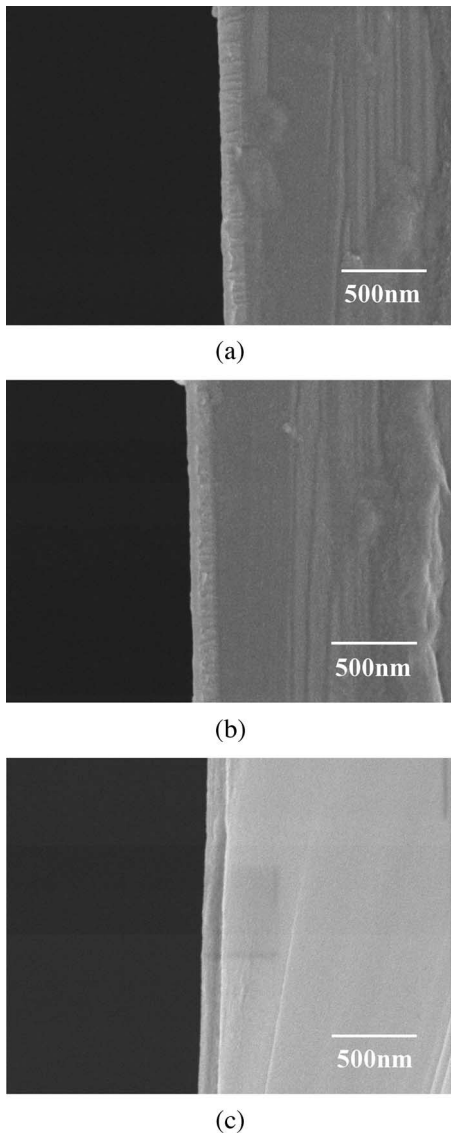

Fig. 3. Cross-sectional field-emission SEM photos of the PIII&D Si–N–O films on silicon substrate. (a) Sample #1. (b) Sample #2. (c) Sample #3.

The cross-sectional field-emission SEM results, which is shown in Fig. 3, indicate that the films have smooth surfaces and have good interfacial transition with silicon substrate, indicating a potentially good adhesion strength. Sample #3 shows a more distinctive interface between the film and substrate compared to the other two samples. No microcracks, peeling, bubbles, and macrodefects can be found in the films or at the interfaces. The film thicknesses indicate that the deposition rates are higher for samples #1 and #2 than sample #3, possibly due to a stronger sputtering effect of the NH_3 plasma [9]. Samples #1 and #2 likely grow in a columnar contour in the oxygen and nitrogen ambient, while sample #3 grows in an equiaxial model in the NH_3 ambient.

The blood-platelet-adhesion behavior is a good indication of blood compatibility as thrombosis is predominately formed by platelet-activation reactions in a complex cascade way [28]. The shape change and spreading of the platelets show the secretion

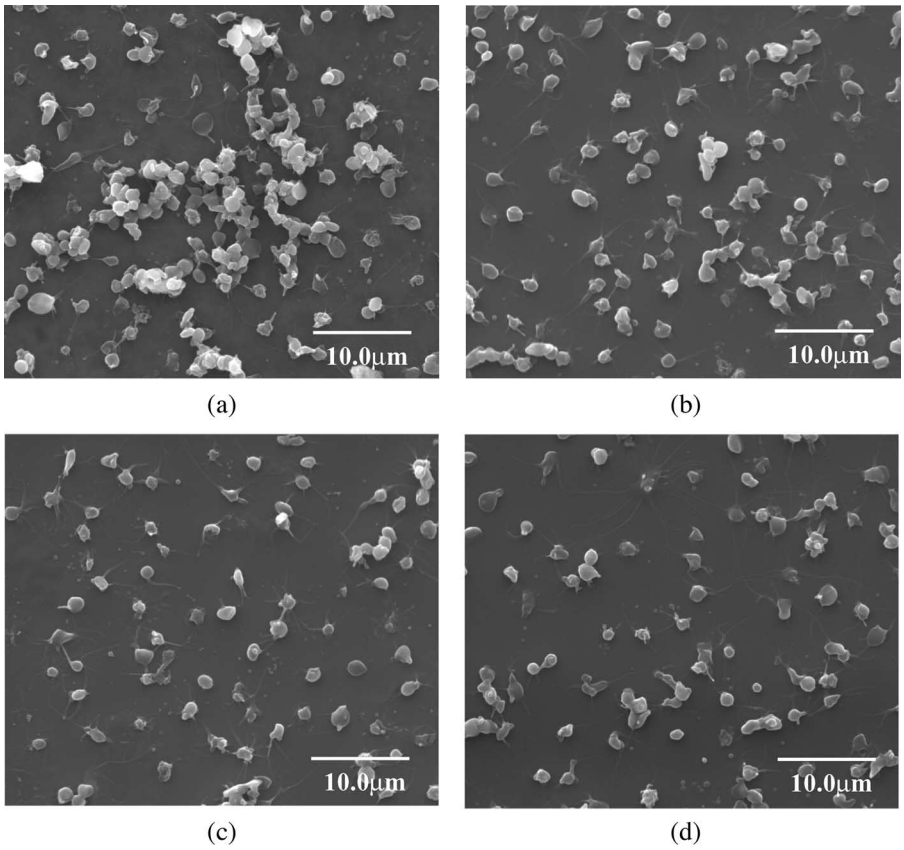

Fig. 4. Morphology of the adherent platelets on: (a) LTIC; (b) sample #1; (c) sample #2; and (d) sample #3.

and release of multiple prothrombotic factors. Therefore, platelet aggregation, pseudopodium, and spreading that are preceding the formation of thrombus are commonly employed to measure the thrombogenicity of the materials [18], [22], [28]. Fig. 4 shows the typical behavior of the adherent platelets on the Si–N–O films and LTIC. On LTIC, apparent aggregation of adhered platelets occurs, and many of them have undergone structural change as manifested by serious pseudopodium and spreading. This phenomenon is typically accompanied by the secretion or synthesis of prothrombotic factors, which activate the platelets [22], [28]. Much less aggregation is observed on the Si–N–O films, although it should be mentioned that all three samples exhibit some degree of pseudopodium, albeit not as severe as that on LTIC. The platelets on samples #2 and #3 exhibit much less pseudopodium, as demonstrated by the isolated and nearly round state, indicating less activation and thrombosis risks. Table III displays the average platelets adherent numbers from ten different viewing fields. The number of adherent platelets on LTIC can only be counted roughly because of heavy aggregation, but is surely much larger than that of Si–N–O films. Among these samples, sample #2 shows the least number.

In addition to the platelet behavior, fibrinogen conformational changes measured by the ELISA method reveal the thrombosis tendency, as the fibrinogen (called the first coagulation factor) conformational change is considered the initial triggering step to stimulate coagulation [22], [28]. The structural changes can be assessed as relative concentrations of the antibody marker for the transformed fibrinogen by measuring the optical density (492 nm). The average values determined from Si–N–O and LTIC are listed in Table III. Fibrinogens adsorbed on LTIC have undergone larger conformational changes than those on the Si–N–O samples. Samples #1 and #2 show obviously smaller values compared to LTIC, and sample #3 shows the least activated states. In general, the trend is consistent with the platelet-adhesion results, indicating that fibrinogen adherence and conformational changes play a critical role in platelet activation and, consequently, the blood compatibility of the biomaterials.

TABLE III
PLATELETS ADHERENT NUMBERS MEASURED BY SEM FROM PLATELET-ADHESION-TESTED SAMPLES (120 min) AND RELATIVE CONCENTRATIONS OF FIBRINOGEN CONFORMATIONALLY TRANSFORMED REPRESENTED BY THE OPTICAL DENSITY IN THE ELISA MEASUREMENT (492 nm)

Samples No.	Platelets adherent number ($\times 10^4/mm^2$)	Fibrinogen transformed number (Relat. Concent.)
LTIC(Control)	7.14(roughly)	2.86±0.1
# 1	5.89±0.03	1.99±0.1
# 2	4.15±0.02	1.96±0.2
# 3	5.53±0.05	0.82±0.08

In order to fathom the interfacial reactions of platelets and fibrinogen with the sample surface, the surface free energy is of great importance from the viewpoint of thermodynamics [29]. Succinctly speaking, platelets provide a surface for the assembly of the prothrombinase complex and secretion or release of the prothrombotic factors [28]. Moreover, the process

TABLE IV
WATER CONTACT ANGLES, SURFACE TENSION AND ITS POLAR AND DISPERSIVE COMPONENTS, AND POLAR CONTRIBUTION RATIO DETERMINED FROM THE Si–N–O FILMS AND LTIC

Sample Nos.	Water contact angle (θ)	γ_s ($mN.m^{-1}$)	γ_s^d ($mN.m^{-1}$)	γ_s^p ($mN.m^{-1}$)	γ_s^p/γ_s
# 1	54.1±2	40.8±0.2	8.37±0.3	32.43±0.9	0.79
# 2	49.2±3	47.0±0.2	23.79±0.4	23.23±1.2	0.49
# 3	49.5±2	49.9±0.1	24.35±0.3	25.53±2.2	0.51
LTIC	78.4±2	44.5±0.3	38.58±0.5	5.83±2.1	0.16

is precipitated by a cleavage of fibrinogen by the serine protease thrombin and subsequent formation of an insoluble polymeric fibrin mesh, which is usually on the surface of the activated platelets acting as an agonist stimulating platelet aggregation and thrombus formation [28], [30]. The surface free energy, which is also represented by surface tension, has an important effect on this process. For instance, polyelectrolytelike fibrinogen consists of hydrophobic and hydrophilic components such as some special amino acids like tyrosine and tryptophane, and a few terminal carboxylate and amino groups, and the hydrophobic amino acids of the protein molecules are mainly located in the interior of the molecules [29]. On a hydrophobic surface, there is an interaction between the hydrophobic component of the fibrinogen and surface, changing the conformation of the molecule from its dissolved or native conformation to the release of activating factors leading to coagulation [29], [30]. This type of interaction is much less significant on a hydrophilic surface, as reported in [29], particularly on some hydrophilic polymers that show less platelet activation [23], [31]. Baier [32] have found that materials with high hydrophilicity and surface tension are likely to be covered by a protein-dominating "conditioning film" that may yield good blood compatibility. Table IV indicates that samples #2 and #3 exhibit the smallest water contact angles and relatively high surface tensions, correlating with the least degree of platelet-activation results. The high surface tensions and hydrophilicity can be attributed to the high polar contribution of the surface energy [32]. Although sample #1 has the highest polar contribution of the surface energy, the much smaller dispersion contribution makes the surface energy lower and more hydrophobic, resulting in poorer platelets adhesion and fibrinogen conformational performance. LTIC is more hydrophobic than our Si–N–O films, showing a very low polar contribution to the surface energy, possibly resulting in stronger interactions with fibrinogen and platelets [30]. Therefore, our relatively hydrophilic Si–N–O films might offer one suitable conditioning surface to make the surface more compatible with blood. The various hydrophilic properties of the films are related to the bonding states such as Si–N and Si–N–O, which contribute more to the higher hydrophilicity than Si–O and Si–Si, according to the results we obtained [9], [10], [17], [27]. However, it should be noted that the surface energy alone may not dictate blood compatibility as thrombogenicity is a very complicated pro cess and far from being well understood. More experiments such as other bioevaluations of toxicity, cell culture, and antibacterial tests are being conducted in our laboratories.

IV. CONCLUSION

We employ a silicon cathodic arc combined with PIII&D to synthesize Si–N–O films. The nitrogen concentrations can be adjusted using different precursors, and the films have good quality. According to the platelet behavior and fibrinogen conformational change, the films have a better blood compatibility than LTIC, making the materials viable in blood-contacting medical products such as bioMEMS, biosensors, and artificial implants.

ACKNOWLEDGMENT

The authors would like to thank T. F. Hung of City University of Hong Kong for the assistance in the field-emission SEM sample preparation and observation.

REFERENCES

[1] F. H. P. M. Habraken and A. E. T. Kuiper, "Silicon nitride and oxynitride films," *Mater. Sci. Eng.*, vol. R12, no. 3, pp. 123–175, Jul. 1994.
[2] E. P. Gusev, H.-C. Lu, E. L. Garfunkel, T. Gustafsson, M. L. Green, and H.-C. Lu, "Growth and characterization of ultrathin nitrided silicon oxide films," *IBM J. Res. Develop.*, vol. 43, no. 3, pp. 265–286, 1999.
[3] R. R. Wang, G. E. Welsch, and O. Monteiro, "Silicon nitride coating on titanium to enable titanium-ceramic bonding," *J. Biomed. Mater. Res.*, vol. 46, no. 2, pp. 262–270, Aug. 1996.
[4] P. R. Hernandez, C. Taboada, L. Leija, V. Tsutsumi, B. Vazquez, F. Valdes-Perezgasga, and J. L. Reyes, "Evaluation of biocompatibility of pH-ISFET materials during long-term subcutaneous implantation," *Sens. Actuators B, Chem.*, vol. 46, no. 2, pp. 133–138, Feb. 1998.
[5] A. C. R. Grayson, R. A. S. Shawgo, A. M. Johnson, N. T. Flynn, Y. Li, M. J. Cima, and R. Langer, "A BioMEMS review: MEMS technology for physiologically integrated devices," *Proc. IEEE*, vol. 92, no. 1, pp. 6–21, Jan. 2004.
[6] R. Kue, A. Sohrabi, D. Nagle, C. Frondoza, and D. Hungerford, "Enhanced proliferation and osteocalcin production by human osteoblast-like MG63 cells on silicon nitride ceramic discs," *Biomaterials*, vol. 20, no. 13, pp. 1195–1201, Jul. 1999.
[7] D. R. Ciarlo, "Silicon nitride thin windows for biomedical microdevices," *Biomed. Microdevices*, vol. 4, no. 1, pp. 63–68, Mar. 2002.
[8] Y. Benmakroha, S. Zhang, and P. Rolfe, "Haemocompatibility of invasive sensors," *Med. Biol. Eng. Comput.*, vol. 33, no. 6, pp. 811–821, Nov. 1995.
[9] G. J. Wan, P. Yang, R. K. Y. Fu, Zh. Q. Yao, N. Huang, and P. K. Chu, "Improvement of nitrogen retained dose using ammonia as a precursor in nitrogen plasma immersion ion implantation of silicon," *J. Vac. Sci. Technol. A, Vac. Surf. Films*, vol. 23, no. 5, pp. 1346–1349, Sep. 2005.
[10] G. J. Wan, R. K. Y. Fu, P. Yang, J. P. Y. Ho, X. Xie, N. Huang, and P. K. Chu, "Surface wettability of nitrogen plasma-implanted silicon," *Nucl. Instrum. Methods Phys. Res. B, Beam Interact. Mater. At.*, vol. 242, no. 1/2, pp. 296–299, Jan. 2006.
[11] G. J. Wan, P. Yang, R. K. Y. Fu, Y. F. Mei, T. Qiu, J. P. Y. Ho, N. Huang, and P. K. Chu, "Characteristics and surface energy of silicon-doped diamond-like carbon films fabricated by plasma immersion ion implantation and deposition," *Diamond Related Mater.*, to be published.
[12] P. K. Chu, B. Y. Tang, L. P. Wang, X. F. Wang, S. Y. Wang, and N. Huang, "Third-generation plasma immersion ion implanter for biomedical materials and research," *Rev. Sci. Instrum.*, vol. 72, no. 3, pp. 1660–1665, Mar. 2001.
[13] Y. Kanda, R. Aoshima, and A. Takada, "Blood compatibility of components and materials in silicon integrated circuits," *Electron. Lett.*, vol. 17, no. 16, pp. 558–559, 1981.
[14] B. A. Weisenberg and D. L. Mooradian, "Hemocompatilility of materials used in microelectromechanical systems: Platelet adhesion and morphology *in vitro*," *J. Biomed. Mater. Res.*, vol. 60, no. 2, pp. 261–283, May 2002.

[15] P. K. Chu, B. Y. Tang, Y. C. Cheng, and P. K. Ko, "Principles and characteristics of a new generation plasma immersion ion implanter," *Rev. Sci. Instrum.*, vol. 68, no. 4, pp. 1866–1874, Apr. 1997.
[16] R. J. Good, "Contact-angle, wetting, and adhesion-A critical-review," *J. Adhes. Sci. Technol.*, vol. 2, no. 6, pp. 1269–1302, 1992.
[17] G. J. Wan, P. Yang, X. J. Shi, M. Wong, H. F. Zhou, N. Huang, and P. K. Chu, "*In vitro* investigation of hemocompatibility of hydrophilic SiN_x:H films fabricated by plasma-enhanced chemical vapor," *Surf. Coat. Technol.*, vol. 200, no. 5/6, pp. 1945–1949, Nov. 2005.
[18] P. Yang, N. Huang, Y. X. Leng, J. Y. Chen, R. K. Y. Fu, S. C. H. Kwok, Y. Leng, and P. K. Chu, "Activation of platelets adhered on amorphous hydrogenated carbon (a-C:H) films synthesized by plasma immersion ion implantation-deposition (PIII-D)," *Biomaterials*, vol. 24, no. 17, pp. 2821–2829, Aug. 2003.
[19] H. Mohri and T. Ohkubo, "Effects of hybrid peptide analogs to receptor recognition domains on a- and y-chains of human fibrinogen on fibrinogen binding to platelets," *Thromb. Haemost.*, vol. 69, no. 5, pp. 490–495, May 1993.
[20] J. M. Gibbins, "Platelet adhesion signaling and the regulation of thrombus formation," *J. Cell Sci.*, vol. 117, no. 16, pp. 3415–3425, Jul. 2004.
[21] T. Groth, E. J. Campbell, K. Herrman, and B. Seifert, "Application of enzyme immune for testing haemocompatibility biomedical polymers," *Biomaterials*, vol. 16, no. 13, pp. 1009–1015, 1995.
[22] A. S. Zhao, P. Yang, Y. X. Leng, H. Sun, J. Wang, G. J. Wan, and N. Huang, "Research on platelet adsorption behavior using enzyme immunoassays and LDH testing," *Key Eng. Mater.*, vol. 288/289, no. 9, pp. 515–520, 2005.
[23] J. F. Moulder, W. F. Stickle, P. E. Sobol, and K. D. Bomben, *Handbook of X-ray Photoelectron Spectroscopy*, J. Chatain, Ed. Eden Prairie, MN: Perkin–Elmer, 1992.
[24] J. Finster, E. D. Klinkenberg, J. Heeg, and W. Braun, "ESCA and SEXAFS investigations of insulating materials for ULSI microelectronic," *Vacuum*, vol. 41, no. 7–9, pp. 1586–1589, 1990.
[25] G. M. Ingo and N. Zacchetti, "XPS investigation on the growth-mode of A-SINX and silicon and nitrogen chemical bondings," *High Temp. Sci.*, vol. 28, pp. 137–151, 1989.
[26] E. Bustarret, M. Bensouda, M. C. Habrard, and J. C. Bruyere, "Configurational statistics in a-$Si_xN_yH_z$ alloys: A quantitative bonding analysis," *Phys. Rev. B, Condens. Matter*, vol. 38, no. 12, pp. 8171–8184, Oct. 1998.
[27] M. Lattemann, E. Nold, S. Ulrich, H. Leiste, and H. Holleck, "Investigation and characterisation of silicon nitride and silicon carbide thin films," *Surf. Coat. Technol.*, vol. 174, pp. 365–369, 2003.
[28] M. B. Gorbet and M. V. Sefton, "Biomaterial-associated thrombosis: Roles of coagulation factors, complement, platelets and leukocytes," *Biomaterials*, vol. 25, no. 26, pp. 5681–5703, Nov. 2004.
[29] B. Ivarsson and I. Lundstrom, "Physical characterization of protein adsorption on metal and metaloxide surfaces," *CRC Crit. Rev. Biocompat.*, vol. 2, no. 1, pp. 1–96, 1986.
[30] S. L. Goodman, K. S. Tweden, and R. M. Albrecht, "Platelet interaction with pyrolytic carbon heart-valve leaflets," *J. Biomed. Mater. Res.*, vol. 32, no. 2, pp. 249–258, Oct. 1996.
[31] L. J. Suggs, J. L. West, and A. G. Mikos, "Platelet adhesion on a bioresorbable poly(propylene fumarate-co-ethylene glycol) copolymer," *Biomaterials*, vol. 20, no. 7, pp. 683–690, Apr. 1999.
[32] R. E. Baier, "Conditioning surfaces to suit the biomedical environment—Recent progress," *J. Biomech. Eng.*, vol. 104, no. 4, pp. 257–271, Nov. 1982.
[33] S. Agathopoulos and P. Nikolopoulos, "Wettability and interfacial interactions in bioceramic-body-liquid systems," *J. Biomed. Mater. Res.*, vol. 29, no. 4, pp. 421–429, Apr. 1995.

Guo Jiang Wan received the B.S. degree in chemical engineering and the M.S. degree in applied electrochemistry from Sichuan University, Chengdu, China, in 1997 and 2000, respectively.

He joined the Southwest Jiaotong University (SWJTU), Chengdu, China, where he is currently an Associate Professor in both materials and biomedical engineering in the College of Materials Science and Engineering and a core member of the Key Laboratory of Advanced Technology for Materials of China Education Ministry in SWJTU. In 2004, he spent a year as a Research Associate with Prof. P. K. Chu's Plasma Laboratory, Department of Physics and Materials Science, City University of Hongkong, Kowloon. His research interests include surface modification, interfacial electrochemistry of biomaterials/tissue, and biocompatibility of blood-contacting biomaterials.

N. Huang, photograph and biography not available at the time of publication.

Sunny C. H. Kwok, photograph and biography not available at the time of publication.

Zh. Y. Shao, photograph and biography not available at the time of publication.

A. S. Zhao, photograph and biography not available at the time of publication.

P. Yang, photograph and biography not available at the time of publication.

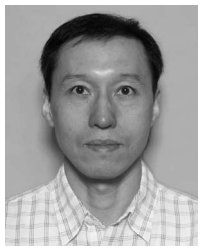

Paul K. Chu (F'03) received the B.S. degree in mathematics from The Ohio State University, Columbus, in 1977 and the M.S. and Ph.D. degrees in chemistry from Cornell University, Ithaca, NY, in 1979 and 1982, respectively.

He joined Charles Evans & Associates in California after graduation and later founded Evans Asia. He joined City University of Hong Kong, Hong Kong, in 1996 and is currently a Professor (Chair) of materials engineering with the Department of Physics and Materials Science. He also holds concurrent Professorships at seven universities and three research institutes in China. His research interests include plasma-processing technology, microelectronics processing, and materials characterization. He has authored/coauthored over 450 journal papers and is the holder of eight U.S. and three Chinese patents.

Prof. Chu is a Fellow of the AVS and HKIE. He is a Senior Editor of the IEEE TRANSACTIONS ON PLASMA SCIENCE and a Guest Editor of *Surface and Coatings Technology*. He serves on the Engineering Panel of the Hong Kong Research Grants Council (RGC). He also serves as a Member of the Editorial Board of *Materials Science and Engineering Reports* and *Nuclear Instruments and Methods in Physics Research B*. He is the Chairman of the International Plasma-Based Ion Implantation Executive Committee and a Member of the International Ion Implantation Technology Executive Committee.